

¹ Memory for television episodes preserves event content
² while introducing new across-event similarities

³ Andrew C. Heusser^{1,2}, Paxton C. Fitzpatrick¹, and Jeremy R. Manning^{1,*}

¹Department of Psychological and Brain Sciences

Dartmouth College, Hanover, NH 03755, USA

²Akili Interactive

Boston, MA 02110

*Corresponding author: jeremy.r.manning@dartmouth.edu

⁴ February 2, 2020

⁵ **Abstract**

The ways our experiences unfold over time define unique *trajectories* through the relevant representational spaces. Within this geometric framework, one can compare the shape of the trajectory formed by an experience to that defined by our later remembering of that experience. We propose a framework for mapping naturalistic experiences onto geometric spaces that characterize how experiences are segmented into discrete events, and how the contents of event sequences evolve over time. We apply this approach to a naturalistic memory experiment which had participants view and recount a television episode. The content of participants' recounts of events from the original episode closely matched the original episode's content. However, the similarity patterns *across* events was much different in the original episode as compared with participants' recounts. We also identified a network of brain structures that are sensitive to the "shapes" of ongoing experiences, and an overlapping network that is sensitive (at the time of encoding) to how people later remembered those experiences in relation to other experiences.

18 In this way, modeling the content of richly structured experiences can reveal how (geometrically
19 and conceptually) those experiences are segmented into events and integrated into our memories
20 of other experiences.

21 **Introduction**

22 What does it mean to *remember* something? In traditional episodic memory experiments (e.g.,
23 list-learning or trial-based experiments; Murdock, 1962; Kahana, 1996), remembering is often cast
24 as a discrete and binary operation: each studied item may be separated from all others, and la-
beled as having been recalled or forgotten. More nuanced studies might incorporate self-reported
25 confidence measures as a proxy for memory strength, or ask participants to discriminate between
26 “recollecting” the (contextual) details of an experience or having a general feeling of “familiarity”
27 (Yonelinas, 2002). Using well-controlled, trial-based experimental designs, the field has amassed
28 a wealth of valuable information regarding human episodic memory. However, there are funda-
29 mental properties of the external world and our memories that trial-based experiments are not well
30 suited to capture (for review also see Koriat and Goldsmith, 1994; Huk et al., 2018). First, our expe-
31 riences and memories are continuous, rather than discrete—removing a (naturalistic) event from
32 the context in which it occurs can substantially change its meaning. Second, the specific language
33 used to describe an experience has little bearing on whether the experience should be considered to
34 have been “remembered.” Asking whether the rememberer has precisely reproduced a specific set
35 of words to describe a given experience is nearly orthogonal to whether they were actually able to
36 remember it. In classic (e.g., list-learning) memory studies, by contrast, the number or proportion
37 of precise recalls is often a primary metric for assessing the quality of participants’ memories.
38 Third, one might remember the *essence* (or a general summary) of an experience but forget (or
39 neglect to recount) particular details. Capturing the essence of what happened is typically the
40 main “point” of recounting a memory to a listener, while the addition of highly specific details
41 may add comparatively little to successful conveyance of an experience.
42

43 How might one go about formally characterizing the “essence” of an experience, or whether

44 it has been recovered by the rememberer? Any given moment of an experience derives meaning
45 from surrounding moments, as well as from longer-range temporal associations (Lerner et al.,
46 2011; Manning, 2019). Therefore, the timecourse describing how an event unfolds is fundamental
47 to its overall meaning. Further, this hierarchy formed by our subjective experiences at different
48 timescales defines a *context* for each new moment (e.g., Howard and Kahana, 2002; Howard et al.,
49 2014), and plays an important role in how we interpret that moment and remember it later (for
50 review see Manning et al., 2015). Our memory systems can leverage these associations to form
51 predictions that help guide our behaviors (Ranganath and Ritchey, 2012). For example, as we
52 navigate the world, the features of our subjective experiences tend to change gradually (e.g., the
53 room or situation we are in at any given moment is strongly temporally autocorrelated), allowing
54 us to form stable estimates of our current situation and behave accordingly (Zacks et al., 2007;
55 Zwaan and Radvansky, 1998).

56 Occasionally, this gradual “drift” of our ongoing experience is punctuated by sudden changes,
57 or “shifts” (e.g., when we walk through a doorway; Radvansky and Zacks, 2017). Prior research
58 suggests that these sharp transitions (termed *event boundaries*) help to discretize our experiences
59 (and their mental representations) into *events* (Radvansky and Zacks, 2017; Brunec et al., 2018;
60 Heusser et al., 2018a; Clewett and Davachi, 2017; Ezzyat and Davachi, 2011; DuBrow and Davachi,
61 2013). The interplay between the stable (within-event) and transient (across-event) temporal
62 dynamics of an experience also provides a potential framework for transforming experiences into
63 memories that distill those experiences down to their essence. For example, prior work has shown
64 that event boundaries can influence how we learn sequences of items (Heusser et al., 2018a; DuBrow
65 and Davachi, 2013), navigate (Brunec et al., 2018), and remember and understand narratives (Zwaan
66 and Radvansky, 1998; Ezzyat and Davachi, 2011). Prior research has implicated the hippocampus
67 and the medial prefrontal cortex as playing a critical role in transforming experiences into structured
68 and consolidated memories (Tompry and Davachi, 2017).

69 Here we sought to examine how the temporal dynamics of a “naturalistic” experience were
70 later reflected in participants’ memories. We analyzed an open dataset that comprised behavioral
71 and functional Magnetic Resonance Imaging (fMRI) data collected as participants viewed and then

72 verbally recounted an episode of the BBC television series *Sherlock* (Chen et al., 2017). We developed
73 a computational framework for characterizing the temporal dynamics of the moment-by-moment
74 content of the episode, and of participants' verbal recalls. Specifically, we use topic modeling (Blei
75 et al., 2003) to characterize the thematic conceptual (semantic) content present in each moment of
76 the episode and recalls, and Hidden Markov Models (Rabiner, 1989; Baldassano et al., 2017) to
77 discretize this evolving semantic content into events. In this way, we cast naturalistic experiences
78 (and recalls of those experiences) as geometric *trajectories* that describe how the experiences evolve
79 over time. Under this framework, successful remembering entails verbally "traversing" the content
80 trajectory of the episode, thereby reproducing the shape (or essence) of the original experience.
81 Comparing the shapes of the topic trajectories of the episode and of participants' retellings of
82 the episode then reveals which aspects of the episode were preserved (or lost) in the translation
83 into memory. We further introduce two novel metrics for assessing memory quality: the *precision*
84 with which a participant recounts each event and 2) the *distinctiveness* of each recall event (relative
85 to other recalled events). We examine how these metrics relate to participants' overall memory
86 performance, and discuss the ways in which they improve upon classic "proportion-recalled"
87 measures for analyzing naturalistic memory. Last, we utilize our framework to identify networks
88 of brain structures whose responses (as participants watched the episode) reflected the temporal
89 dynamics of the episode, and how participants would later recount it.

90 Results

91 To characterize the "essence" of the *Sherlock* episode and participants' subsequent recounts of
92 its unfolding, we used a topic model (Blei et al., 2003) to discover the latent themes in the episode's
93 dynamic content. Topic models take as inputs a vocabulary of words to consider and a collection
94 of text documents, and return two output matrices. The first of these is a *topics matrix* whose rows
95 are topics (latent themes) and whose columns correspond to words in the vocabulary. The entries
96 of the topics matrix define how each word in the vocabulary is weighted by each discovered topic.
97 For example, a detective-themed topic might weight heavily on words like "crime," and "search."

98 The second output is a *topic proportions matrix*, with one row per document and one column per
99 topic. The topic proportions matrix describes what mixture of discovered topics is reflected in each
100 document.

101 Chen et al. (2017) collected hand-annotated information about each of 1000 (manually identified)
102 scenes spanning the roughly 50 minute video used in their experiment. This information included:
103 a brief narrative description of what was happening; whether the scene took place indoors or
104 outdoors; the names of any characters on the screen; the names of any characters who were in
105 focus in the camera shot; the names of characters who were speaking; the location where the scene
106 took place; the camera angle (close up, medium, long, etc.); whether or not background music was
107 present; and other similar details (for a full list of annotated features see *Methods*). We took from
108 these annotations the union of all unique words (excluding stop words, such as “and,” “or,” “but,”
109 etc.) across all features and scenes as the “vocabulary” for the topic model. We then concatenated
110 the sets of words across all features contained in overlapping, 50-scene sliding windows, and
111 treated each 50-scene sequence as a single “document” for the purpose of fitting the topic model.
112 Next, we fit a topic model with (up to) $K = 100$ topics to this collection of documents. We found that
113 32 unique topics (with non-zero weights) were sufficient to describe the time-varying content of the
114 video (see *Methods*; Figs. 1, S2). Note that our approach is similar in some respects to Dynamic Topic
115 Models (Blei and Lafferty, 2006) in that we sought to characterize how the thematic content of the
116 episode evolved over time. However, whereas Dynamic Topic Models are designed to characterize
117 how the properties of *collections* of documents change over time, our sliding window approach
118 allows us to examine the topic dynamics within a single document (or video). Specifically, our
119 approach yielded (via the topic proportions matrix) a single *topic vector* for each timepoint of the
120 episode (we set timepoints to match the acquisition times of the 1976 fMRI volumes collected as
121 participants viewed the episode).

122 The topics we found were heavily character-focused (e.g., the top-weighted word in each topic
123 was nearly always a character) and could be roughly divided into themes that were primarily
124 Sherlock Holmes-focused (Sherlock is the titular character), primarily John Watson-focused (John
125 is Sherlock’s close confidant and assistant), or focused on Sherlock and John interacting (Fig. S2).

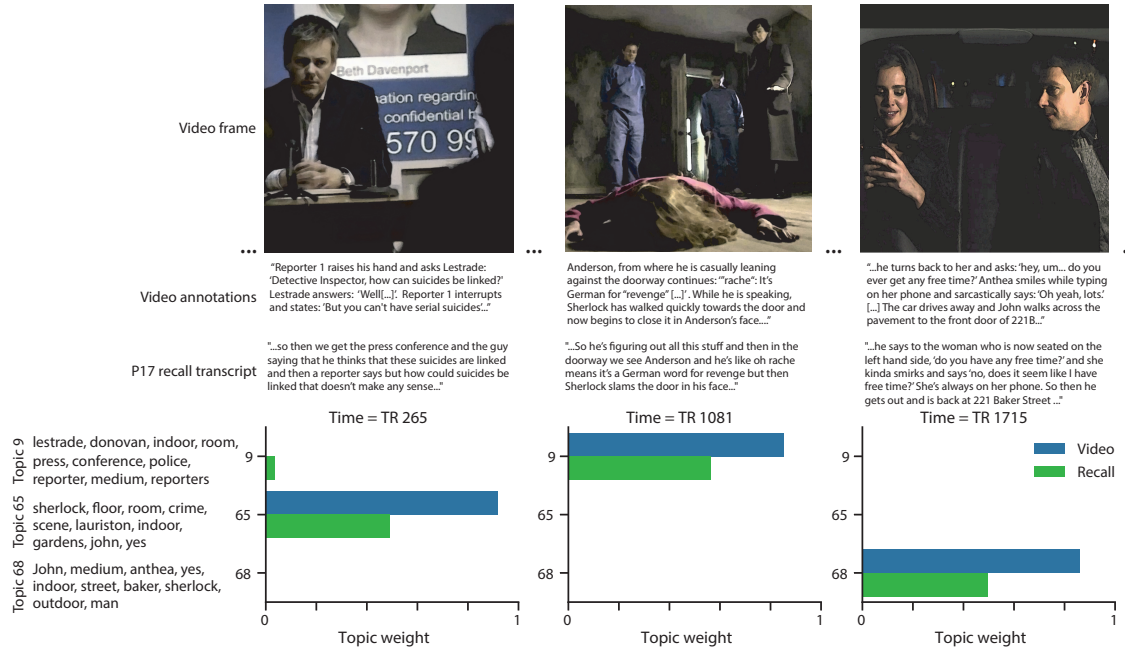


Figure 1: Methods overview. We used hand-annotated descriptions of each moment of video to fit a topic model. Three example video frames and their associated descriptions are displayed (top two rows). Participants later recalled the video (in the third row, we show example recalls of the same three scenes from participant 13). We used the topic model (fit to the annotations) to estimate topic vectors for each moment of video and each sentence the participants recalled. Example topic vectors are displayed in the bottom row (blue: video annotations; green: example participant’s recalls). Three topic dimensions are shown (the highest-weighted topics for each of the three example scenes, respectively). We also show the ten highest-weighted words for each topic. Figure S2 provides a full list of the top 10 words from each of the discovered topics.

126 Several of the topics were highly similar, which we hypothesized might allow us to distinguish
127 between subtle narrative differences (if the distinctions between those overlapping topics were
128 meaningful; also see Fig. S3). The topic vectors for each timepoint were *sparse*, in that only a small
129 number (usually one or two) of topics tended to be “active” in any given timepoint (Fig. 2A).
130 Further, the dynamics of the topic activations appeared to exhibit *persistence* (i.e., given that a
131 topic was active in one timepoint, it was likely to be active in the following timepoint) along with
132 *occasional rapid changes* (i.e., occasionally topics would appear to spring into or out of existence).
133 These two properties of the topic dynamics may be seen in the block diagonal structure of the
134 timepoint-by-timepoint correlation matrix (Fig. 2B) and reflect the gradual drift and sudden shifts
135 fundamental to the contextual dynamics of real-world experiences. Given this observation, we
136 adapted an approach devised by Baldassano et al. (2017), and used a Hidden Markov Model (HMM)
137 to identify the *event boundaries* where the topic activations changed rapidly (i.e., at the boundaries
138 of the blocks in the correlation matrix; event boundaries identified by the HMM are outlined in
139 yellow). Part of our model fitting procedure required selecting an appropriate number of “events”
140 to segment the timeseries into. We used an optimization procedure to identify the number of
141 events that maximized within-event stability while also minimizing across-event correlations (see
142 *Methods* for additional details). To create a stable “summary” of the video, we computed the
143 average topic vector within each event (Fig. 2C).

144 Given that the time-varying content of the video could be segmented cleanly into discrete
145 events, we wondered whether participants’ recalls of the video also displayed a similar structure.
146 We applied the same topic model (already trained on the video annotations) to each participant’s
147 recalls. Analogous to how we analyzed the time-varying content of the video, to obtain similar
148 estimates for participants’ recalls, we treated each (overlapping) 10-sentence “window” of their
149 transcript as a “document” and then computed the most probable mix of topics reflected in each
150 timepoint’s sentences. This yielded, for each participant, a number-of-windows by number-of-
151 topics topic proportions matrix that characterized how the topics identified in the original video
152 were reflected in the participant’s recalls. Note that an important feature of our approach is
153 that it allows us to compare participant’s recalls to events from the original video, despite that



Figure 2: Modelling naturalistic stimuli and recalls. All panels: darker colors indicate greater values; range: [0, 1]. **A.** Topic vectors ($K = 100$) for each of the 1976 video timepoints. **B.** Timepoint-by-timepoint correlation matrix of the topic vectors displayed in Panel A. Event boundaries detected by the HMM are denoted in yellow (30 events detected). **C.** Average topic vectors for each of the 30 video events. **D.** Topic vectors for each of 265 sliding windows of sentences spoken by an example participant while recalling the video. **E.** Timepoint-by-timepoint correlation matrix of the topic vectors displayed in Panel D. Event boundaries detected by the HMM are denoted in yellow (22 events detected). **F.** Average topic vectors for each of the 22 recalled events from the example participant. **G.** Correlations between the topic vectors for every pair of video events (Panel C) and recalled events (from the example participant; Panel F). For similar plots for all participants see Figure S5. **H.** Average correlations between each pair of video events and recalled events (across all 17 participants). To create the figure, each recalled event was assigned to the video event with the most correlated topic vector (yellow boxes in panels G and H). The heat maps in each panel were created using Seaborn (Waskom et al., 2016).

¹⁵⁴ different participants may have used different language to describe the same event, and that those
¹⁵⁵ descriptions may not match the original annotations. This is a substantial benefit of projecting
¹⁵⁶ the video and recalls into a shared “topic” space. An example topic proportions matrix from one
¹⁵⁷ participant’s recalls is shown in Figure 2D.

¹⁵⁸ Although the example participant’s recall topic proportions matrix has some visual similarity to
¹⁵⁹ the video topic proportions matrix, the time-varying topic proportions for the example participant’s
¹⁶⁰ recalls are not as sparse as for the video (e.g., compare Figs. 2A and D). Similarly, although there
¹⁶¹ do appear to be periods of stability in the recall topic dynamics (e.g., most topics are active or
¹⁶² inactive over contiguous blocks of time), the overall timecourses are not as cleanly delineated as
¹⁶³ the video topics are. To examine these patterns in detail, we computed the timepoint-by-timepoint
¹⁶⁴ correlation matrix for the example participant’s recall topic proportions (Fig. 2E). As in the video
¹⁶⁵ correlation matrix (Fig. 2B), the example participant’s recall correlation matrix has a strong block
¹⁶⁶ diagonal structure, indicating that their recalls are discretized into separated events. As for the
¹⁶⁷ video correlation matrix, we can use an HMM, along with the aforementioned number-of-events
¹⁶⁸ optimization procedure (also see *Methods*) to determine how many events are reflected in the
¹⁶⁹ participant’s recalls and where specifically the event boundaries fall (outlined in yellow). We
¹⁷⁰ carried out a similar analysis on all 17 participants’ recall topic proportions matrices (Fig. S4).

¹⁷¹ Two clear patterns emerged from this set of analyses. First, although every individual partic-
¹⁷² ipant’s recalls could be segmented into discrete events (i.e., every individual participant’s recall
¹⁷³ correlation matrix exhibited clear block diagonal structure; Fig. S4), each participant appeared to
¹⁷⁴ have a unique *recall resolution*, reflected in the sizes of those blocks. For example, some participants’
¹⁷⁵ recall topic proportions segmented into just a few events (e.g., Participants P4, P5, and P7), while
¹⁷⁶ others’ recalls segmented into many shorter duration events (e.g., Participants P12, P13, and P17).
¹⁷⁷ This suggests that different participants may be recalling the video with different levels of detail-
¹⁷⁸ e.g., some might touch on just the major plot points, whereas others might attempt to recall every
¹⁷⁹ minor scene or action. The second clear pattern present in every individual participant’s recall
¹⁸⁰ correlation matrix is that, unlike in the video correlation matrix, there are substantial off-diagonal
correlations. Whereas each event in the original video was (largely) separable from the others

182 (Fig. 2B), in transforming those separable events into memory, participants appear to be integrating
183 across multiple events, blending elements of previously recalled and not-yet-recalled events
184 into each newly recalled event (Figs. 2D, S4; also see Manning et al., 2011; Howard et al., 2012).

185 The above results indicate that both the structure of the original video and participants' recalls
186 of the video exhibit event boundaries that can be identified automatically by characterizing the
187 dynamic content using a shared topic model and segmenting the content into events using HMMs.
188 Next, we asked whether some correspondence might be made between the specific content of the
189 events the participants experienced in the video, and the events they later recalled. One approach
190 to linking the experienced (video) and recalled events is to label each recalled event as matching
191 the video event with the most similar (i.e., most highly correlated) topic vector (Figs. 2G, S5). This
192 yields a sequence of "presented" events from the original video, and a (potentially differently
193 ordered) sequence of "recalled" events for each participant. Analogous to classic list-learning
194 studies, we can then examine participants' recall sequences by asking which events they tended
195 to recall first (probability of first recall; Fig. 3A; Welch and Burnett, 1924; Postman and Phillips,
196 1965; Atkinson and Shiffrin, 1968); how participants most often transition between recalls of the
197 events as a function of the temporal distance between them (lag-conditional response probability;
198 Fig. 3B; Kahana, 1996); and which events they were likely to remember overall (serial position
199 recall analyses; Fig. 3C; Murdock, 1962). Interestingly, for two of these analyses (probability of first
200 recall and lag-conditional response probability curves) we observe patterns comparable to classic
201 effects from the list-learning literature: namely, a higher probability of initiating recall with the
202 first event in the sequence (Fig. 3A) and a higher probability of transitioning to neighboring events
203 with an asymmetric forward bias (Fig. 3C). In contrast, we do not observe a pattern comparable to
204 the serial position effect (Fig. 3C), but rather we see higher memory for specific events distributed
205 somewhat evenly throughout the video.

206 We can also apply two list-learning-native analyses that describe how participants group items
207 in their recall sequences: temporal clustering and semantic clustering (Polyn et al., 2009, see
208 *Methods* for details). Temporal clustering refers to the extent to which participants group their
209 recall responses according to encoding position. Overall, we found that sequentially viewed video

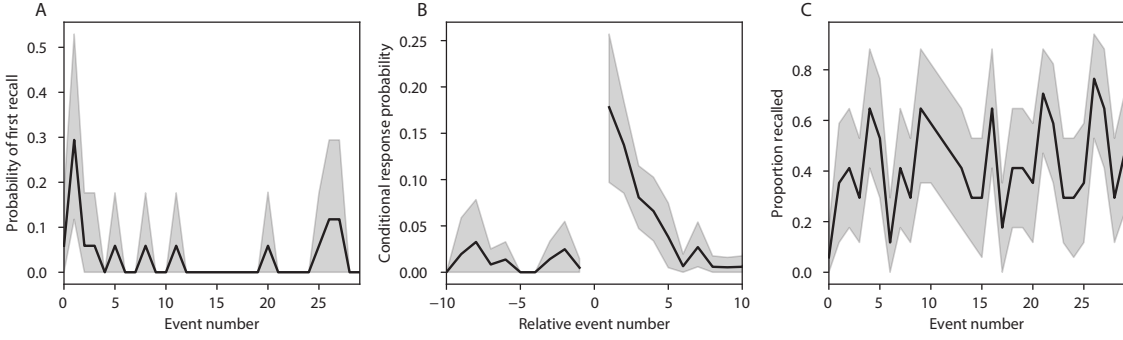


Figure 3: Naturalistic extensions of classic list-learning memory analyses. A. The probability of first recall as a function of the serial position of the event in the video. B. The probability of recalling each event, conditioned on having most recently recalled the event *lag* events away in the video. C. The proportion of participants who recalled each event, as a function of the serial position of the events in the video. All panels: error bars denote bootstrap-estimated standard error of the mean.

events were clustered heavily in participants' recall event sequences (mean: 0.767, SEM: 0.029), and that participants with higher temporal clustering scores tended to perform better according to both Chen et al. (2017)'s hand-annotated memory scores (Pearson's $r(15) = 0.62$, $p = 0.008$) and our model's estimate (Pearson's $r(15) = 0.54$, $p = 0.024$). Semantic clustering measures the extent to which participants cluster their recall responses according to semantic similarity. We found that participants tended to recall semantically similar video events together (mean: 0.787, SEM: 0.018), and that semantic clustering score was also related to both hand-annotated (Pearson's $r(15) = 0.65$, $p = 0.004$) and model-derived (Pearson's $r(15) = 0.63$, $p = 0.007$) memory performance.

Statistical models of memory studies often treat memory recalls as binary (e.g. the item was recalled or not) and independent events. However, our framework produces a content-based model of individual stimulus and recall events, allowing for direct quantitative comparison between all stimulus and recall events, as well as between the recall events themselves. Leveraging these content-based models of the stimulus/recall events, we developed two novel metrics for quantifying naturalistic memory representations: *precision* and *distinctiveness*. We define precision as the average correlation between the topic proportions of each recall event and the maximally correlated video event (Fig. 4). Participants whose recall events are more veridical descriptions of what

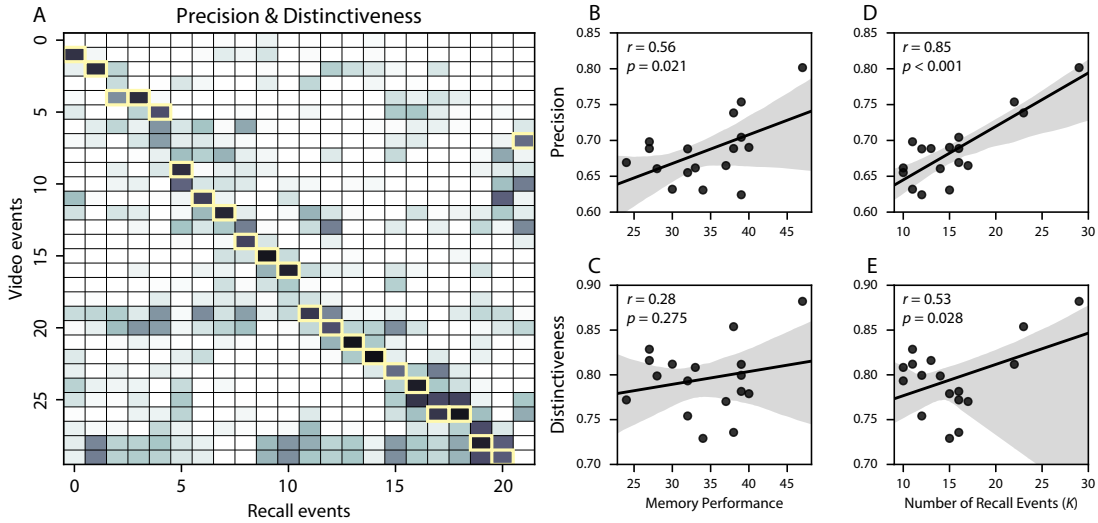


Figure 4: Novel content-based metrics of naturalistic memory: precision and distinctiveness. **A.** A video-recall correlation matrix for a representative participant (17). The yellow boxes highlight the maximum correlation in each column. Precision was computed as the average of the maximum correlation in each column. On the other hand, distinctiveness was defined as the average of everything except for the maximum correlation in each column. **B.** The (Pearson's) correlation between precision and hand-annotated memory performance. **C.** The correlation between precision and the number of events recovered by the model (k). **D.** The correlation between distinctiveness and hand-annotated memory performance. **E.** The correlation between distinctiveness and the number of events recovered by the model (k).

happened in the video event will presumably have higher precision scores. We find that, across participants, a higher precision score is correlated to both hand-annotated memory performance (Pearson's $r(15) = 0.56, p = 0.021$) and the number of recall events estimated by our model (Pearson's $r(15) = 0.85, p < 0.001$). A second novel metric we introduce here is distinctiveness, or how unique the recall description was to each video event. We define distinctiveness as 1 minus the average of all non-matching recall events from the video-recall correlation matrix. We hypothesized that participants who recounted events in a more distinctive way would display better overall memory. We find that this distinctiveness score is related to our model's estimated number of recalled events (Pearson's $r(15) = 0.49, p = 0.046$) but not to the analogous hand-annotated metric (Pearson's $r(15) = 0.31, p = 0.23$). In summary, using two novel metrics afforded by our approach, we find that participants whose recalls are both more precise and distinct remember more content.

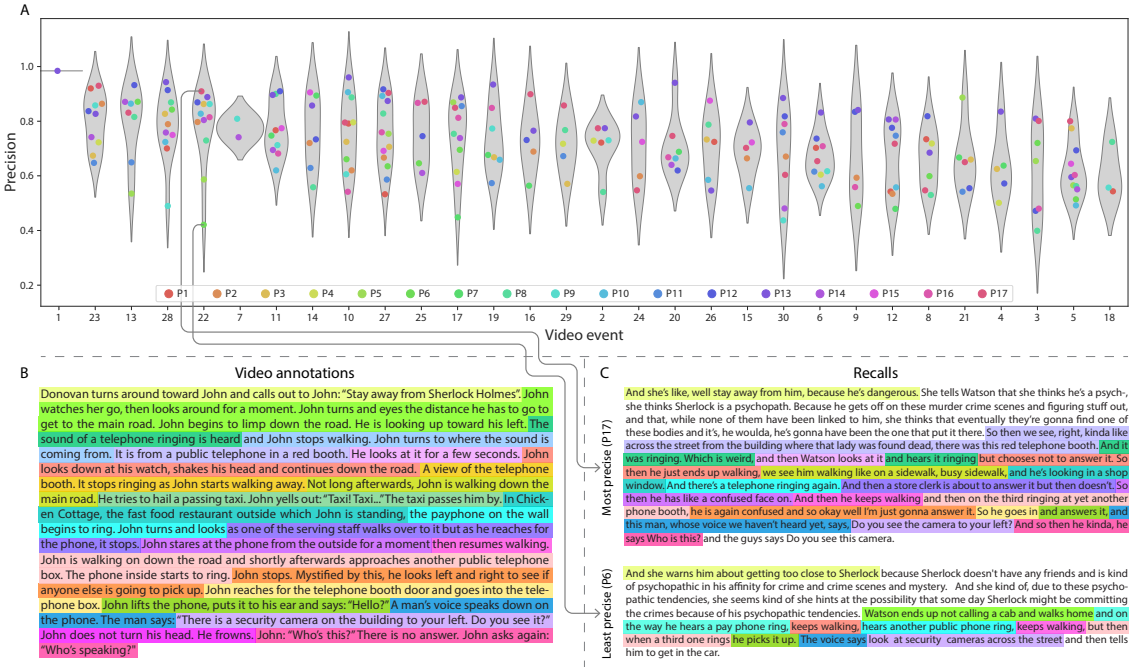


Figure 5: Precision metric reflects completeness of recall. **A.** Recall precision distributions over participants, for each video event. Grey violin plots display kernel density estimates for the distribution of recall precision scores for a single video event. Colored dots within the violin plots represent individual participants' recall precision for that event. Video events are ordered along the x-axis by the average precision with which they were remembered. **B.** The set of "Narrative Details" video annotations (generated by Chen et al., 2017) for scenes comprising an example video event (22) identified by the HMM. Each action or feature is highlighted in a different color. **C.** A subset of the sentences comprising the most precise (P17) and least precise (P6) participants' recalls of video event 22. Descriptions of specific actions or features reflecting those highlighted in panel B are highlighted in the corresponding color.

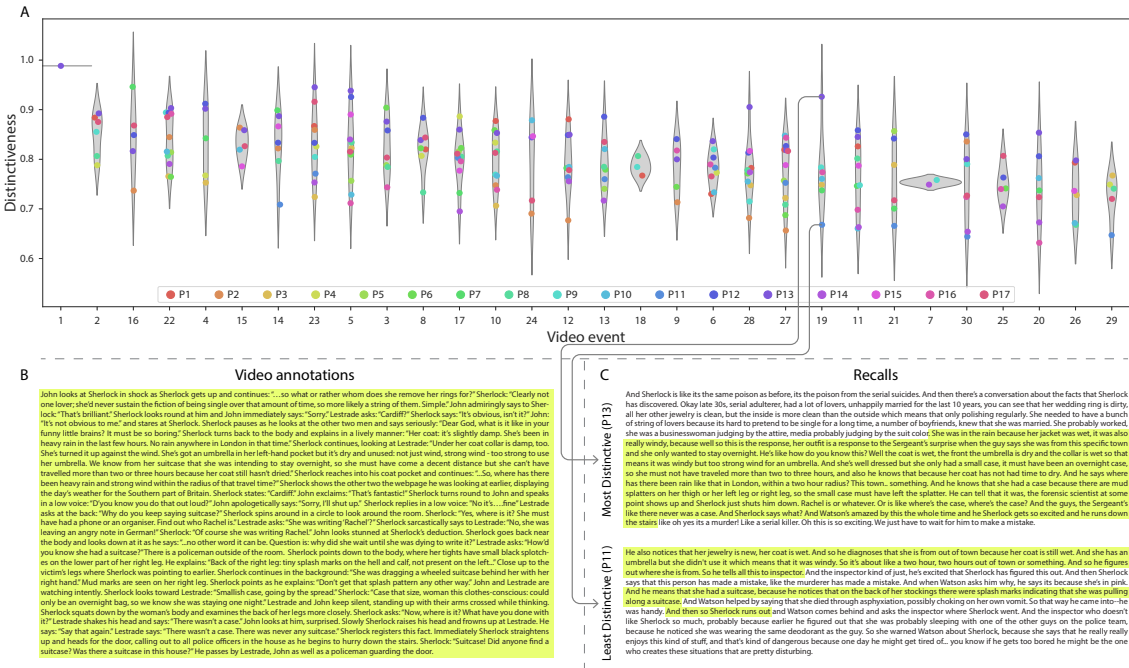


Figure 6: Distinctiveness metric reflects specificity of recall. A. Recall distinctiveness distributions over participants, for each video event. Kernel density estimates for each video event’s distribution of recall distinctiveness scores, analogous to Fig. 5A. B. The set of “Narrative Details” video annotations (generated by Chen et al., 2017) for scenes comprising an example video event (19) identified by the HMM. C. The sentences comprising the most distinctive (P13) and least distinctive (P11) participants’ recalls of video event 19. Descriptions of recalled content specific to video event 19 (as opposed to that combining surrounding events) are highlighted.

238 The prior analyses leverage the correspondence between the 100-dimensional topic proportion
239 matrices for the video and participants' recalls to characterize recall. However, it is difficult to gain
240 deep insights into that content solely by examining the topic proportion matrices (e.g., Figs. 2A,
241 D) or the corresponding correlation matrices (Figs. 2B, E, S4). To visualize the time-varying
242 high-dimensional content in a more intuitive way (Heusser et al., 2018b) we projected the topic
243 proportions matrices onto a two-dimensional space using Uniform Manifold Approximation and
244 Projection (UMAP; McInnes et al., 2018). In this lower-dimensional space, each point represents a
245 single video or recall event, and the distances between the points reflect the distances between the
246 events' associated topic vectors (Fig. 7). In other words, events that are near to each other in this
247 space are more semantically similar.

248 Visual inspection of the video and recall topic trajectories reveals a striking pattern. First,
249 the topic trajectory of the video (which reflects its dynamic content; Fig. 7A) is captured nearly
250 perfectly by the averaged topic trajectories of participants' recalls (Fig. 7B). To assess the consistency
251 of these recall trajectories across participants, we asked: given that a participant's recall trajectory
252 had entered a particular location in topic space, could the position of their *next* recalled event
253 be predicted reliably? For each location in topic space, we computed the set of line segments
254 connecting successively recalled events (across all participants) that intersected that location (see
255 *Methods* for additional details). We then computed (for each location) the distribution of angles
256 formed by the lines defined by those line segments and a fixed reference line (the *x*-axis). Rayleigh
257 tests revealed the set of locations in topic space at which these across-participant distributions
258 exhibited reliable peaks (blue arrows in Fig. 7B reflect significant peaks at $p < 0.05$, corrected). We
259 observed that the locations traversed by nearly the entire video trajectory exhibited such peaks.
260 In other words, participants exhibited similar trajectories that also matched the trajectory of the
261 original video (Fig. 7C). This is especially notable when considering the fact that the number of
262 events participants recalled (dots in Fig. 7C) varied considerably across people, and that every
263 participant used different words to describe what they had remembered happening in the video.
264 Differences in the numbers of remembered events appear in participants' trajectories as differences
265 in the sampling resolution along the trajectory. We note that this framework also provides a

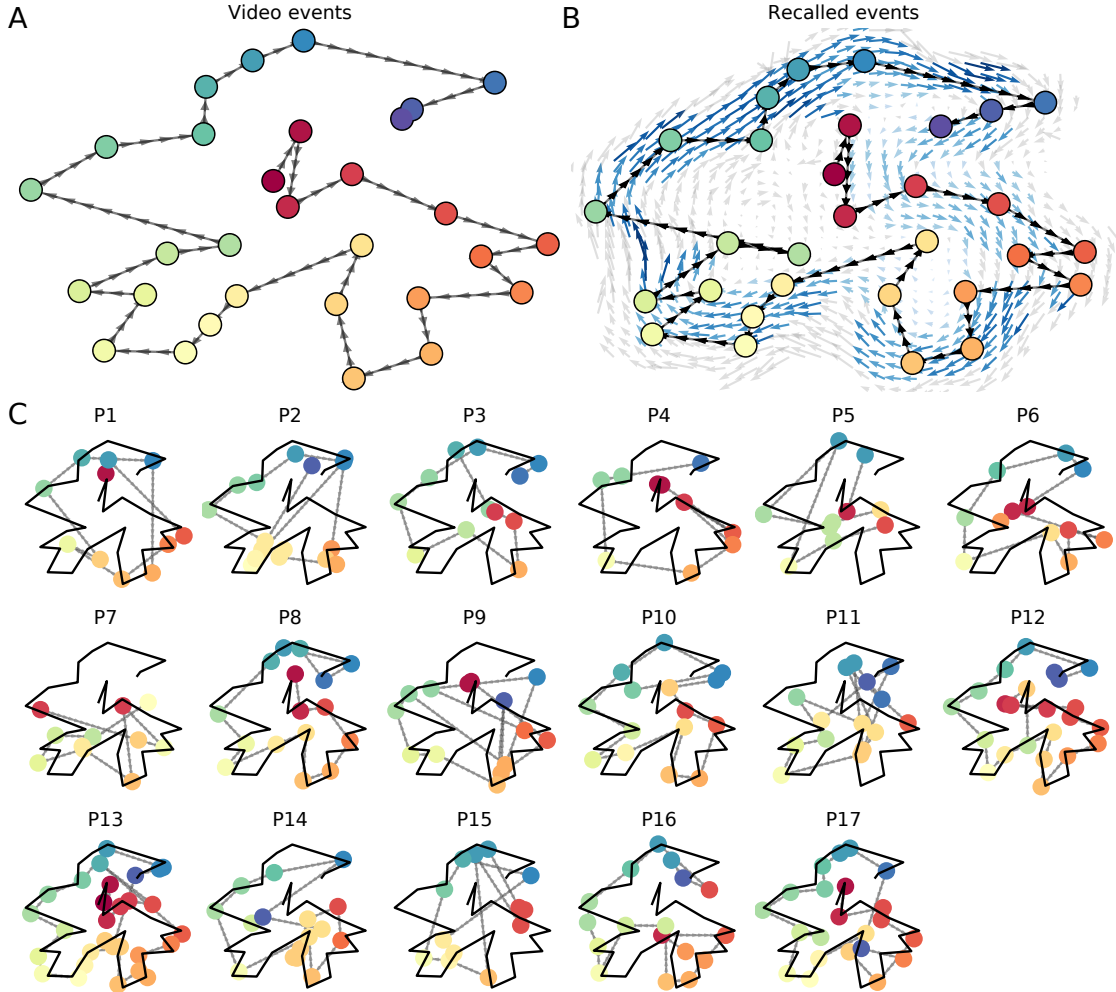


Figure 7: Trajectories through topic space capture the dynamic content of the video and recalls. All panels: the topic proportion matrices have been projected onto a shared two-dimensional space using UMAP. **A.** The two-dimensional topic trajectory taken by the episode of *Sherlock*. Each dot indicates an event identified using the HMM (see *Methods*); the dot colors denote the order of the events (early events are in red; later events are in blue), and the connecting lines indicate the transitions between successive events. **B.** The average two-dimensional trajectory captured by participants' recall sequences, with the same format and coloring as the trajectory in Panel A. To compute the event positions, we matched each recalled event with an event from the original video (see *Results*), and then we averaged the positions of all events with the same label. The arrows reflect the average transition direction through topic space taken by any participants whose trajectories crossed that part of topic space; blue denotes reliable agreement across participants via a Rayleigh test ($p < 0.05$, corrected). **C.** The recall topic trajectories (gray) taken by each individual participant (P1–P17). The video's trajectory is shown in black for reference. (Same format and coloring as Panel A.)

means of detangling classic “proportion recalled” measures (i.e., the proportion of video events referenced in participants’ recalls) from participants’ abilities to recapitulate the full shape of the original video (i.e., the similarity in the shape of the original video trajectory and that defined by each participant’s recounting of the video).

Because our analysis framework projects the dynamic video content and participants’ recalls onto a shared topic space, and because the dimensions of that space are known (i.e., each topic dimension is a set of weights over words in the vocabulary; Fig. S2), we can examine the topic trajectories to understand which specific content was remembered well (or poorly). For each video event, we can ask: what was the average correlation (across participants) between the video event’s topic vector and the closest matching recall event topic vectors from each participant? This yields a single correlation coefficient for each video event, describing how closely participants’ recalls of the event tended to reliably capture its content (Fig. 8A). Given this summary of which events were recalled reliably (or not), we next asked whether the better-remembered or worse-remembered events tended to reflect particular topics. We computed a weighted average of the topic vectors for each video event, where the weights reflected how reliably each event was recalled. To visualize the result, we created a “wordle” image (Mueller et al., 2018) where words weighted more heavily by better-remembered topics appear in a larger font (Fig. 8B, green box). Across the full video, content that reflected topics necessary to convey the central focus of the video (e.g., the names of the two main characters, “Sherlock” and “John”, and the address of a major recurring location, “221B Baker Street”) were best remembered. An analogous analysis revealed which themes were poorly remembered. Here in computing the weighted average over events’ topic vectors, we weighted each event in *inverse* proportion to how well it was remembered (Fig. 8B, red box). The least well-remembered video content reflected information not necessary to conveying the video’s “gist,” such as the proper names of relatively minor characters (e.g., “Mike,” “Molly,” and “Lestrade”) and locations (e.g., “St. Bartholomew’s Hospital”), as well as the brief, animated clip participants viewed at the beginning of each of the two scan session (involving “singing” “cartoon” characters).

A similar result emerged from assessing the topic vectors for individual video and recall events (Fig. 8C). Here, for each of the three best- and worst-remembered video events, we have constructed

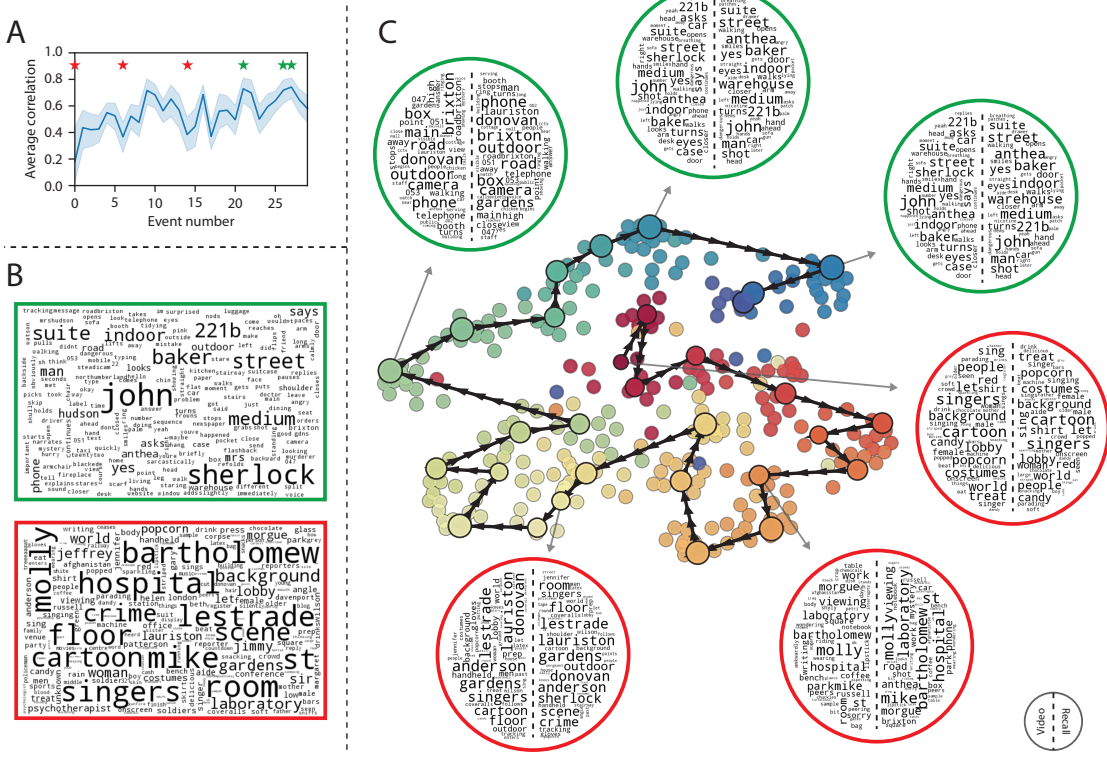


Figure 8: Transforming experience into memory. **A.** Average correlations (across participants) between the topic vectors from each video event and the closest-matching recall events. Error bars denote bootstrap-derived across-participant 95% confidence intervals. The stars denote the three best-remembered events (green) and worst-remembered events (red). **B.** Wordles comprising the top 200 highest-weighted words reflected in the weighted-average topic vector across video events. Green: video events were weighted by how well the topic vectors derived from recalls of those events matched the video events' topic vectors (Panel A). Red: video events were weighted by the inverse of how well their topic vectors matched the recalled topic vectors. **C.** The set of all video and recall events is projected onto the two-dimensional space derived in Figure 7. The dots outlined in black denote video events (dot size reflects the average correlation between the video event's topic vector and the topic vectors from the closest matching recalled events from each participant; bigger dots denote stronger correlations). The dots without black outlines denote recalled events. All dots are colored using the same scheme as Figure 7A. Wordles for several example events are displayed (green: three best-remembered events; red: three worst-remembered events). Within each circular wordle, the left side displays words associated with the topic vector for the video event, and the right side displays words associated with the (average) recall event topic vector, across all recall events matched to the given video event.

294 two wordles: one from the original video event's topic vector (left) and a second from the average
295 recall topic vector for that event (right). The three best-remembered events (circled in green)
296 correspond to scenes important to the central plot-line: a mysterious figure spying on John in a
297 phone booth; John and Sherlock discussing the murders in their apartment; and Sherlock laying a
298 trap to catch the murderer. Meanwhile, the three worst-remembered events (circled in red) reflect
299 scenes that are non-essential to summarizing the narrative's structure: the two appearances of
300 singing cartoon characters; Molly watching as Sherlock beats a corpse in the morgue; and Sherlock
301 noticing evidence of Anderson's and Donovan's affair.

302 The results thus far inform us about which aspects of the dynamic content in the episode
303 participants watched were preserved or altered in participants' memories of the episode. We next
304 carried out a series of analyses aimed at understanding which brain structures might implement
305 these processes. In one analysis we sought to identify which brain structures were sensitive
306 to the video's dynamic content, as characterized by its topic trajectory. Specifically, we used a
307 searchlight procedure to identify the extent to which each cluster of voxels exhibited a timecourse
308 of activity (as the participants watched the video) whose temporal correlation matrix matched
309 the temporal correlation matrix of the original video's topic proportions (Fig. 2B). As shown
310 in Figure 10A, the analysis revealed a network of regions including bilateral frontal cortex and
311 cingulate cortex, suggesting that these regions may play a role in processing information relevant
312 to the narrative structure of the video. In a second analysis, we sought to identify which brain
313 structures' responses (while viewing the video) reflected how each participant would later *recall*
314 the video. We used an analogous searchlight procedure to identify clusters of voxels whose
315 temporal correlation matrices reflected the temporal correlation matrix of the topic proportions for
316 each individual's recalls (Figs. 2D, S4). As shown in Figure 10B, the analysis revealed a network of
317 regions including the ventromedial prefrontal cortex (vmPFC), anterior cingulate cortex (ACC), and
318 right medial temporal lobe (rMTL), suggesting that these regions may play a role in transforming
319 each individual's experience into memory. In identifying regions whose responses to ongoing
320 experiences reflect how those experiences will be remembered later, this latter analysis extends
321 classic *subsequent memory analyses* (e.g., Paller and Wagner, 2002) to domain of naturalistic stimuli.

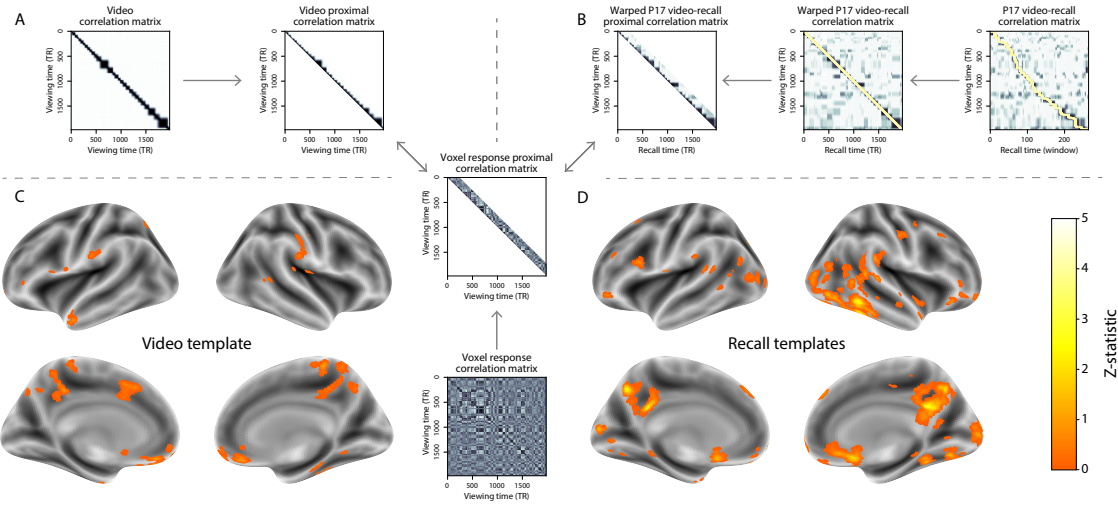


Figure 9: Brain structures that underlie the transformation of experience into memory. **A.** We searched for regions whose responses (as participants watched the video) matched the temporal correlation matrix of the video topic proportions. These regions are sensitive to the narrative structure of the video. **B.** We searched for regions whose responses (as participants watched the video) matched the temporal correlation matrix of the topic proportions derived from each individual's later recall of video. These regions are sensitive to how the narrative structure of the video is transformed into a memory of the video. Both panels: the maps are thresholded at $p < 0.05$, corrected.

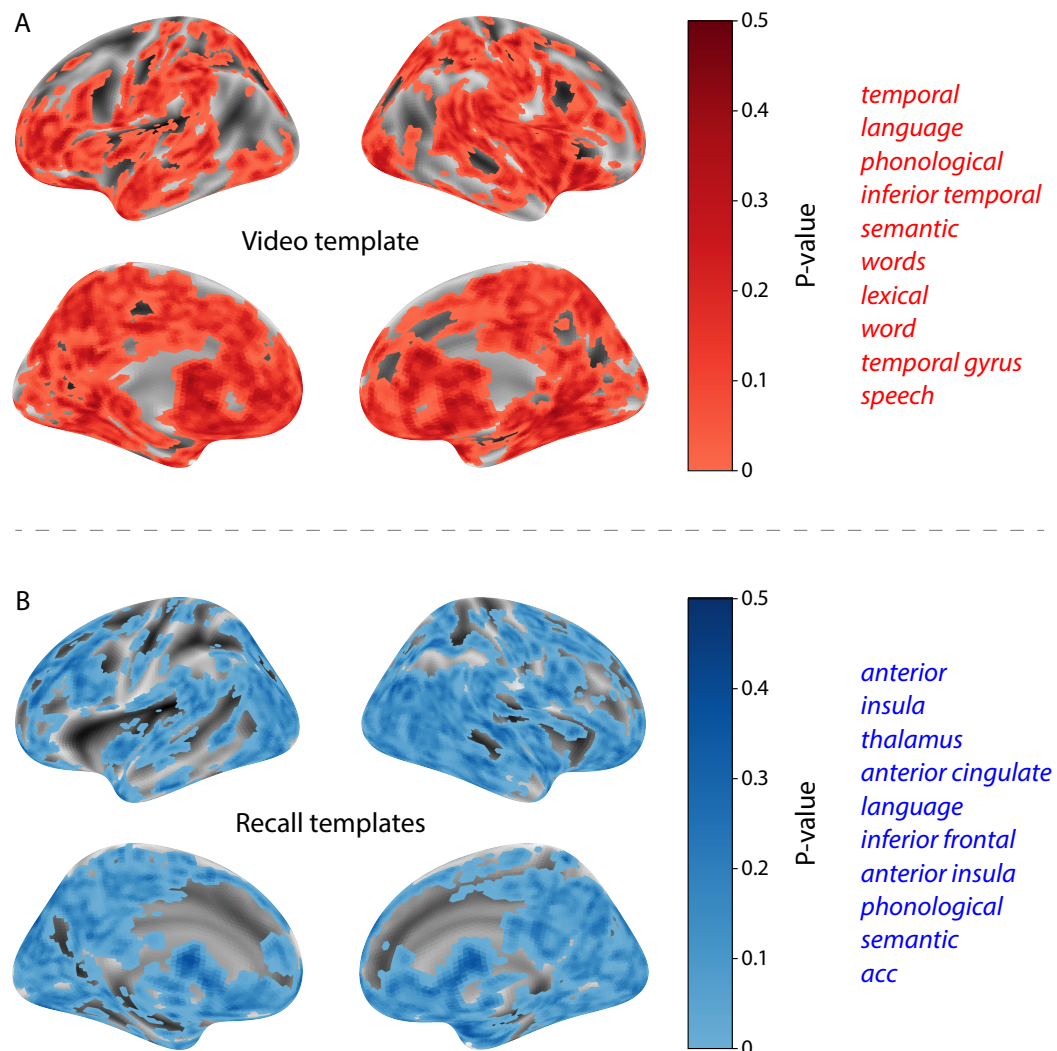


Figure 10: INSERT CAPTION HERE

322 **Discussion**

323 Our work casts remembering as reproducing (behaviorally and neurally) the topic trajectory, or
324 shape, of an experience. This view draws inspiration from prior work aimed at elucidating
325 the neural and behavioral underpinnings of how we process dynamic naturalistic experiences
326 and remember them later. One approach to identifying neural responses to naturalistic stimuli
327 (including experiences) entails building a model of the stimulus and searching for brain regions
328 whose responses are consistent with the model. In prior work, a series of studies from Uri
329 Hasson's group (Lerner et al., 2011; Simony et al., 2016; Chen et al., 2017; Baldassano et al., 2017;
330 Zadbood et al., 2017) have extended this approach with a clever twist: rather than building an
331 explicit stimulus model, these studies instead search for brain responses (while experiencing the
332 stimulus) that are reliably similar across individuals. So called *inter-subject correlation* (ISC) and
333 *inter-subject functional connectivity* (ISFC) analyses effectively treat other people's brain responses
334 to the stimulus as a "model" of how its features change over time. By contrast, in our present
335 work we used topic models and HMMs to construct an explicit stimulus model (i.e., the topic
336 trajectory of the video). When we searched for brain structures whose responses are consistent
337 with the video's topic trajectory, we identified a network of structures that overlapped strongly
338 with the "long temporal receptive window" network reported by the Hasson group (e.g., compare
339 our Fig. 10A with the map of long temporal receptive window voxels in Lerner et al., 2011). This
340 provides support for the notion that part of the long temporal receptive window network may be
341 maintaining an explicit model of the stimulus dynamics. When we performed a similar analysis
342 after swapping out the video's topic trajectory with the recall topic trajectories of each individual
343 participant, this allowed us to identify brain regions whose responses (as the participants viewed
344 the video) reflected how the video trajectory would be transformed in memory (as reflected by
345 the recall topic trajectories). The analysis revealed that the rMTL and vmPFC may play a role in
346 this person-specific transformation from experience into memory. The role of the MTL in episodic
347 memory encoding has been well-reported (e.g., Paller and Wagner, 2002; Davachi et al., 2003;
348 Ranganath et al., 2004; Davachi, 2006; Wiltgen and Silva, 2007; Diana et al., 2007; van Kesteren

349 et al., 2013). Prior work has also implicated the medial prefrontal cortex in representing “schema”
350 knowledge (i.e., general knowledge about the format of an ongoing experience given prior similar
351 experiences; van Kesteren et al., 2012, 2013; Schlichting and Preston, 2015; Gilboa and Marlatte,
352 2017; Spalding et al., 2018). Integrating across our study and this prior work, one interpretation is
353 that the person-specific transformations mediated (or represented) by the rMTL and vmPFC may
354 reflect schema knowledge being leveraged, formed, or updated, incorporating ongoing experience
355 into previously acquired knowledge.

356 In extending classical free recall analyses to our naturalistic memory framework, we recovered
357 two patterns of recall dynamics central to list-learning studies: a high probability of initiating
358 recall with the first video event (Fig. 3A) and a strong bias toward transitioning from recalling a
359 given event to recalling the event immediately following it (Fig. 3B). However, equally noteworthy
360 are the typical free recall results not recovered in these analyses, as each highlights a fundamental
361 difference between list-learning studies and naturalistic memory paradigms like the one employed
362 in the present study. The most noticeable departure from hallmark free recall dynamics in these
363 findings is the apparent lack of a serial position effect in Figure 3C, which instead shows greater
364 and lesser recall probabilities for events distributed across the video stimulus. Stimuli in free recall
365 experiments most often comprise lists of simple, common words, presented to participants in a
366 random order. (In fact, numerous word pools have been developed based on these criteria; e.g.,
367 Friendly et al., 1982). These stimulus qualities enable two assumptions that are central to word
368 list analyses, but frequently do not hold for real-world experiences. First, researchers conducting
369 free recall studies may assume that the content at each presentation index is essentially equal, and
370 does not bear qualities that would cause participants to remember it more or less successfully than
371 others. Such is rarely the case with real-world experiences or experiments meant to approximate
372 them, and the effects of both intrinsic and observer-dependent factors on stimulus memorability
373 are well established (for review see Chun and Turk-Browne, 2007; Bylinskii et al., 2015; Tyng
374 et al., 2017). Second, the random ordering of list items ensures that (across participants, on
375 average) there is no relationship between the thematic similarity of individual stimuli and their
376 presentation positions—in other words, two semantically related words are no more likely to be

377 presented next to each other than at opposite ends of the list. In most cases, the exact opposite
378 is true of real-world episodes. Our internal thoughts, our actions, and the physical state of the
379 world around us all tend to follow a direct, causal progression. As a result, each moment of our
380 experience tends to be inherently more similar to surrounding moments than to those in the distant
381 past or future. Memory literature has termed this strong temporal autocorrelation “context,” and
382 in various media that depict real-world events (e.g., movies and written stories), we recognize
383 it as a *narrative structure*. While a random word list (by definition) has no such structure, the
384 logical progression between ideas and actions in a naturalistic stimulus prompts the rememberer
385 to recount presented events in order, starting with the beginning. This tendency is reflected in our
386 findings’ second departure from typical free recall dynamics: a lack of increased probability of first
387 recall for end-of-sequence events (Fig. 3A).

388 Thus, analyses such as those in Figure 3 that address only the temporal dynamics of free re-
389 call paint an incomplete picture of memory for naturalistic episodes. While useful for studying
390 presentation order-dependent recall dynamics, they neglect to consider the stimuli’s content (or,
391 for example, that content’s potential interrelatedness). However, sensitivity to stimulus and recall
392 content introduces a new challenge: distinguishing between levels of recall quality for a stimulus
393 (i.e., an event) that is considered to have been “remembered.” When modeling memory experi-
394 ments, often times events (or items) and their later memories are treated as binary and independent
395 events (e.g., a given list item was simply either remembered or not remembered). Various models
396 of memory (e.g., Yonelinas, 2002) attempt to improve upon this by including confidence ratings,
397 rendering this binary judgement instead categorical. Our novel framework allows one to assess
398 memory performance in a more continuous way (*precision*), as well as analyze the correlational
399 structure of each encoding event to each memory event (*distinctiveness*). Further and importantly,
400 these two novel metrics we introduce here arise from comparisons of the actual content of the
401 experience/memories, which is not typically modeled. Leveraging this, we find that the successful
402 memory performance is related to 1) the precision with which the participant recounts each event
403 and 2) the distinctiveness of each recall event (relative to the other recalled events). The first finding
404 suggests that the information retained for *any individual event* may predict the overall amount of

405 information retained by the participant. The second finding suggests that the ability to distin-
406 guish between temporally or semantically similar content is also related to the quantity of content
407 recovered. Intriguingly, prior studies show that pattern separation, or the ability to discriminate
408 between similar experiences, is impaired in many cognitive disorders as well as natural aging
409 (Stark et al., 2010; Yassa et al., 2011; Yassa and Stark, 2011). Future work might explore whether
410 and how these metrics compare between cognitively impoverished groups and healthy controls.

411 While a large number of language models exist (e.g., WAS, LSA, word2vec, universal sentence
412 encoder; Steyvers et al., 2004; Landauer et al., 1998; Mikolov et al., 2013; Cer et al., 2018), here
413 we use latent dirichlet allocation (LDA)-based topic models for a few reasons. First, topic models
414 capture the *essence* of a text passage devoid of the specific set and order of words used. This
415 was an important feature of our model since different people may accurately recall a scene using
416 very different language. Second, words can mean different things in different contexts (e.g. “bat”
417 as the act of hitting a baseball, the object used for that action, or as a flying mammal). Topic
418 models are robust to this, allowing words to exist as part of multiple topics. Last, topic models
419 provide a straightforward means to recover the weights for the particular words comprising a topic,
420 enabling easy interpretation of an event’s contents (e.g. Fig. 8). Other models such as Google’s
421 universal sentence encoder offer a context-sensitive encoding of text passages, but the encoding
422 space is complex and non-linear, and thus recovering the original words used to fit the model is
423 not straightforward. However, it’s worth pointing out that our framework is divorced from the
424 particular choice of language model. Moreover, many of the aspects of our framework could be
425 swapped out for other choices. For example, the language model, the timeseries segmentation
426 model and the video-recall matching function could all be customized for the particular problem.
427 Indeed for some problems, recovery of the particular recall words may not be necessary, and thus
428 other text-modeling approaches (such as universal sentence encoder) may be preferable. Future
429 work will explore the influence of particular model choices on the framework’s accuracy.

430 Our work has broad implications for how we characterize and assess memory in real-world
431 settings, such as the classroom or physician’s office. For example, the most commonly used
432 classroom evaluation tools involve simply computing the proportion of correctly answered exam

433 questions. Our work indicates that this approach is only loosely related to what educators might
434 really want to measure: how well did the students understand the key ideas presented in the
435 course? Under this typical framework of assessment, the same exam score of 50% could be
436 ascribed to two very different students: one who attended the full course but struggled to learn
437 more than a broad overview of the material, and one who attended only half of the course but
438 understood the material perfectly. Instead, one could apply our computational framework to build
439 explicit content models of the course material and exam questions. This approach would provide
440 a more nuanced and specific view into which aspects of the material students had learned well
441 (or poorly). In clinical settings, memory measures that incorporate such explicit content models
442 might also provide more direct evaluations of patients' memories.

443 Methods

444 Experimental design and data collection

445 Data were collected by Chen et al. (2017). In brief, participants ($n = 17$) viewed the first 48 minutes
446 of "A Study in Pink", the first episode of the BBC television series *Sherlock*, while fMRI volumes
447 were collected (TR = 1500 ms). The stimulus was divided into a 23 min (946 TR) and a 25 min
448 (1030 TR) segment to mitigate technical issues related to the scanner. After finishing the clip,
449 participants were instructed to (quoting from Chen et al., 2017) "describe what they recalled of the
450 [episode] in as much detail as they could, to try to recount events in the original order they were
451 viewed in, and to speak for at least 10 minutes if possible but that longer was better. They were told
452 that completeness and detail were more important than temporal order, and that if at any point
453 they realized they had missed something, to return to it. Participants were then allowed to speak
454 for as long as they wished, and verbally indicated when they were finished (e.g., 'I'm done')."
455 For additional details about the experimental procedure and scanning parameters, see Chen et al.
456 (2017). The experimental protocol was approved by Princeton University's Institutional Review
457 Board.

458 After preprocessing the fMRI data and warping the images into a standard (3 mm³ MNI) space,
459 the voxel activations were z-scored (within voxel) and spatially smoothed using a 6 mm (full width
460 at half maximum) Gaussian kernel. The fMRI data were also cropped so that all video-viewing
461 data were aligned across participants. This included a constant 3 TR (4.5 s) shift to account for the
462 lag in the hemodynamic response. (All of these preprocessing steps followed Chen et al., 2017,
463 where additional details may be found.)

464 **Data and code availability**

465 The fMRI data we analyzed are available online [here](#). The behavioral data and all of our analysis
466 code may be downloaded [here](#).

467 **Statistics**

468 All statistical tests we performed were two-sided.

469 **Modeling the dynamic content of the video and recall transcripts**

470 **Topic modeling**

471 The input to the topic model we trained to characterize the dynamic content of the video comprised
472 998 hand-generated annotations of short (mean: 2.96s) scenes spanning the video clip (Chen et al.,
473 2017 generated 1000 annotations total; we removed two referring to the break between the first and
474 second scan sessions, during which no fMRI data was collected). The features annotated included:
475 narrative details (a sentence or two describing what happened in that scene); whether the scene
476 took place indoors or outdoors; names of any characters that appeared in the scene; name(s) of
477 characters in camera focus; name(s) of characters who were speaking in the scene; the location (in
478 the story) that the scene took place; camera angle (close up, medium, long, top, tracking, over the
479 shoulder, etc.); whether music was playing in the scene or not; and a transcription of any on-screen
480 text. We concatenated the text for all of these features within each segment, creating a “bag of
481 words” describing each scene. We then re-organized the text descriptions into overlapping sliding

482 windows of 50 scenes each. In other words, we created a “context” for each scene comprising the
483 text descriptions of the preceding 25 scenes, the present scene, and the following 24 scenes. To
484 model the “context” at the beginning and end of the video (i.e., within 25 scenes of the beginning or
485 end), we created overlapping sliding windows that grew in size from one scene to the full length,
486 then similarly tapered their length at the end. This bore the additional benefit of representing each
487 scene’s description in the text corpus an equal number of times.

488 We trained our model using these overlapping text samples with `scikit-learn` (version 0.19.1;
489 Pedregosa et al., 2011), called from our high-dimensional visualization and text analysis software,
490 `HyperTools` (Heusser et al., 2018b). Specifically, we used the `CountVectorizer` class to transform
491 the text from each window into a vector of word counts (using the union of all words across all
492 scenes as the “vocabulary,” excluding English stop words); this yielded a number-of-windows
493 by number-of-words *word count* matrix. We then used the `LatentDirichletAllocation` class
494 (`topics=100, method='batch'`) to fit a topic model (Blei et al., 2003) to the word count matrix,
495 yielding a number-of-windows (1047) by number-of-topics (100) *topic proportions* matrix. The
496 topic proportions matrix describes which mix of topics (latent themes) is present in and around
497 each scene. Next, we transformed the topic proportions matrix to match the 1976 fMRI volume
498 acquisition times. We assigned each topic vector to the timepoint midway between the beginning
499 of the first scene and the end of the last scene in its corresponding sliding text window. We
500 then transformed these timepoints to units of TRs and interpolated the dynamic topic proportions
501 matrix to obtain number-of-TRs (1976) by number-of-topics (100) matrix.

502 We created similar topic proportions matrices using hand-annotated transcripts of each partici-
503 pant’s recall of the video (annotated by Chen et al., 2017). We tokenized the transcript into a list of
504 sentences, and then re-organized the list into overlapping sliding windows spanning 10 sentences
505 each (and analogously tapered the lengths of the first and last 10 sliding windows). In turn, we
506 transformed each window’s sentences into a word count vector (using the same vocabulary as for
507 the video model). We then used the topic model already trained on the video scenes to compute
508 the most probable topic proportions for each sliding window. This yielded a number-of-windows
509 (range: 83–312) by number-of-topics (100) topic proportions matrix for each participant. These

510 reflected the dynamic content of each participant's recalls. Note: for details on how we selected the
511 video and recall window lengths and number of topics, see *Supporting Information* and Figure S1.

512 **Parsing topic trajectories into events using Hidden Markov Models**

513 We parsed the topic trajectories of the video and participants' recalls into events using Hidden
514 Markov Models (Rabiner, 1989). Given the topic proportions matrix (describing the mix of topics
515 at each timepoint) and a number of states, K , an HMM recovers the set of state transitions that
516 segments the timeseries into K discrete states. Following Baldassano et al. (2017), we imposed an
517 additional set of constraints on the discovered state transitions that ensured that each state was
518 encountered exactly once (i.e., never repeated). We used the BrainIAK toolbox (Capota et al., 2017)
519 to implement this segmentation.

520 We used an optimization procedure to select the appropriate K for each topic proportions
521 matrix. Prior studies on narrative structure and processing have shown that we both perceive
522 and internally represent the world around us at multiple, hierarchical timescales (e.g., Hasson
523 et al., 2008; Lerner et al., 2011; Hasson et al., 2015; Chen et al., 2017; Baldassano et al., 2017, 2018).
524 However, for the purposes of our framework, we sought to identify the single timescale of event-
525 representations that is emphasized *most heavily* in the temporal structure of the video and each
526 participant's recalls. We quantified this as the set of K event boundaries that yielded the maximal
527 distinctiveness between the content (i.e., topics) within each event and that in all other events.
528 Specifically, we computed (for each matrix)

$$\operatorname{argmax}_K [W_1(a, b)],$$

529 where a was the distribution of correlations between the topic vectors of timepoints within the
530 same state and b was the average correlation between the topic vectors of timepoints within
531 *different* states. For each possible K , we computed the first Wasserstein distance (W_1 ; also known as
532 "earth mover's distance"; Dobrushin, 1970; Ramdas et al., 2017) between these distributions, and
533 chose the K -value that yielded the greatest difference. Figure 2B displays the event boundaries

534 returned for the video, and Figure S4 displays the event boundaries returned for each participant's
535 recalls (See Fig. S6 for the optimization functions for the video and recalls). After obtaining these
536 event boundaries, we created stable estimates of each topic proportions matrix by averaging the
537 topic vectors within each event. This yielded a number-of-events by number-of-topics matrix for
538 the video and recalls from each participant.

539 **Naturalistic extensions of classic list-learning analyses**

540 In traditional list-learning experiments, participants view a list of items (e.g., words) and then recall
541 the items later. Our video-recall event matching approach affords us the ability to analyze memory
542 in a similar way. The video and recall events can be treated analogously to studied and recalled
543 "items" in a list-learning study. We can then extend classic analyses of memory performance and
544 dynamics (originally designed for list-learning experiments) to the more naturalistic video recall
545 task used in this study.

546 Perhaps the simplest and most widely used measure of memory performance is *accuracy*—i.e.,
547 the proportion of studied (experienced) items (in this case, the 30 video events) that the participant
548 later remembered. Chen et al. (2017) developed a human rating system whereby the quality of
549 each participant's memory was evaluated by an independent rater. We found a strong across-
550 participants correlation between these independant ratings and the overall number of events that
551 our HMM approach identified in participants' recalls (Pearson's $r(15) = 0.65, p = 0.004$).

552 As described below, we next considered a number of memory performance measures that are
553 typically associated with list-learning studies. We also provide a software package, Quail, for
554 carrying out these analyses (Heusser et al., 2017).

555 **Probability of first recall (PFR).** PFR curves (Welch and Burnett, 1924; Postman and Phillips,
556 1965; Atkinson and Shiffrin, 1968) reflect the probability that an item will be recalled first as a
557 function of its serial position during encoding. To carry out this analysis, we initialized a number-
558 of-participants (17) by number-of-video-events (30) matrix of zeros. Then for each participant, we
559 found the index of the video event that was recalled first (i.e., the video event whose topic vector

560 was most strongly correlated with that of the first recall event) and filled in that index in the matrix
561 with a 1. Finally, we averaged over the rows of the matrix, resulting in a 1 by 30 array representing
562 the proportion of participants that recalled an event first, as a function of the order of the event's
563 appearance in the video (Fig. 3A).

564 **Lag conditional probability curve (lag-CRP).** The lag-CRP curve (Kahana, 1996) reflects the
565 probability of recalling a given event after the just-recalled event, as a function of their relative
566 positions (or *lag*). In other words, a lag of 1 indicates that a recalled event came immediately after
567 the previously recalled event in the video, and a lag of -3 indicates that a recalled event came 3
568 events before the previously recalled event. For each recall transition (following the first recall),
569 we computed the lag between the current recall event and the next recall event, normalizing by
570 the total number of possible transitions. This yielded a number-of-participants (17) by number-
571 of-lags (-29 to +29; 61 lags total) matrix. We averaged over the rows of this matrix to obtain a
572 group-averaged lag-CRP curve (Fig. 3B).

573 **Serial position curve (SPC).** SPCs (Murdock, 1962) reflect the proportion of participants that
574 remember each item as a function of the items' serial position during encoding. We initialized
575 a number-of-participants (17) by number-of-video-events (30) matrix of zeros. Then, for each
576 recalled event, for each participant, we found the index of the video event that the recalled event
577 most closely matched (via the correlation between the events' topic vectors) and entered a 1 into
578 that position in the matrix (i.e., for the given participant and event). This resulted in a matrix
579 whose entries indicated whether or not each event was recalled by each participant (depending
580 on whether the corresponding entires were set to one or zero). Finally, we averaged over the rows
581 of the matrix to yield a 1 by 30 array representing the proportion of participants that recalled each
582 event as a function of the order of the event's appearance in the video (Fig. 3C).

583 **Temporal clustering scores.** Temporal clustering describes participants' tendency to organize
584 their recall sequences by the learned items' encoding positions. For instance, if a participant
585 recalled the video events in the exact order they occurred (or in exact reverse order), this would

586 yield a score of 1. If a participant recalled the events in random order, this would yield an expected
587 score of 0.5. For each recall event transition (and separately for each participant), we sorted
588 all not-yet-recalled events according to their absolute lag (i.e., distance away in the video). We
589 then computed the percentile rank of the next event the participant recalled. We averaged these
590 percentile ranks across all of the participant’s recalls to obtain a single temporal clustering score
591 for the participant.

592 **Semantic clustering scores.** Semantic clustering describes participants’ tendency to recall seman-
593 tically similar presented items together in their recall sequences. Here, we used the topic vectors
594 for each event as a proxy for its semantic content. Thus, the similarity between the semantic
595 content for two events can be computed by correlating their respective topic vectors. For each
596 recall event transition, we sorted all not-yet-recalled events according to how correlated the topic
597 vector of *the closest-matching video event* was to the topic vector of the closest-matching video event
598 to the just-recalled event. We then computed the percentile rank of the observed next recall. We
599 averaged these percentile ranks across all of the participant’s recalls to obtain a single semantic
600 clustering score for the participant.

601 **Novel naturalistic memory metrics**

602 **Precision.** We tested whether participants who recalled more events were also more *precise* in
603 their recollections. For each participant, we computed the average correlation between the topic
604 vectors for each recall event and those of its closest-matching video event. This gave a single value
605 per participant representing the average precision across all recalled events. We then Fisher’s *z*-
606 transformed these values and correlated them with both hand-annotated and model-derived (i.e.,
607 k or the number of events recovered by the HMM) memory performance.

608 **Distinctiveness.** We also considered the *distinctiveness* of each recalled event. That is, how
609 uniquely a recalled event’s topic vector matched a given video event topic vector, versus the
610 topic vectors for the other video events. We hypothesized that participants with high memory

611 performance might describe each event in a more distinctive way (relative to those with lower
612 memory performance who might describe events in a more general way). To test this hypothesis
613 we define a distinctiveness score for each recall event as

$$d(\text{event}) = 1 - \bar{c}(\text{event}),$$

614 where $\bar{c}(\text{event})$ is the average correlation between the given recalled event's topic vector and the
615 topic vectors from all video events *except* the best-matching video event. We then averaged these
616 distinctiveness scores across all of the events recalled by the given participant. As above, we used
617 Fisher's *z*-transformation before correlating these values with hand-annotated and model derived
618 memory performance scores across-subjects.

619 **Visualizing the video and recall topic trajectories**

620 We used the UMAP algorithm (McInnes et al., 2018) to project the 100-dimensional topic space
621 onto a two-dimensional space for visualization (Figs. 7, 8). Importantly, to ensure that all of
622 the trajectories were projected onto the *same* lower dimensional space, we computed the low-
623 dimensional embedding on a "stacked" matrix created by vertically concatenating the events-
624 by-topics topic proportions matrices for the video, across-participants average recalls and all 17
625 individual participants' recalls. We then divided the rows of the result (a total-number-of-events
626 by two matrix) back into separate matrices for the video topic trajectory and the trajectories for
627 each participant's recalls (Fig. 7). This general approach for discovering a shared low-dimensional
628 embedding for a collections of high-dimensional observations follows Heusser et al. (2018b). Note:
629 for further details on how we created this low-dimensional embedding space, see *Supporting
630 Information*.

631 **Estimating the consistency of flow through topic space across participants**

632 In Figure 7B, we present an analysis aimed at characterizing locations in topic space that dif-
633 ferent participants move through in a consistent way (via their recall topic trajectories). The

634 two-dimensional topic space used in our visualizations (Fig. 7) comprised a 60×60 (arbitrary
635 units) square. We tiled this space with a 50×50 grid of evenly spaced vertices, and defined a
636 circular area centered on each vertex whose radius was two times the distance between adjacent
637 vertices (i.e., 2.4 units). For each vertex, we examined the set of line segments formed by connecting
638 each pair successively recalled events, across all participants, that passed through this circle. We
639 computed the distribution of angles formed by those segments and the x -axis, and used a Rayleigh
640 test to determine whether the distribution of angles was reliably “peaked” (i.e., consistent across
641 all transitions that passed through that local portion of topic space). To create Figure 7B we drew
642 an arrow originating from each grid vertex, pointing in the direction of the average angle formed
643 by line segments that passed within its circular radius. We set the arrow lengths to be inversely
644 proportional to the p -values of the Rayleigh tests at each vertex. Specifically, for each vertex we
645 converted all of the angles of segments that passed within 2.4 units to unit vectors, and we set
646 the arrow lengths at each vertex proportional to the length of the (circular) mean vector. We also
647 indicated any significant results ($p < 0.05$, corrected using the Benjamani-Hochberg procedure) by
648 coloring the arrows in blue (darker blue denotes a lower p -value, i.e., a longer mean vector); all
649 tests with $p \geq 0.05$ are displayed in gray and given a lower opacity value.

650 **Searchlight fMRI analyses**

651 In Figure 10, we present two analyses aimed at identifying brain regions whose responses (as par-
652 ticipants viewed the video) exhibited a particular temporal structure. We developed a searchlight
653 analysis wherein we constructed a cube centered on each voxel (radius: 5 voxels) and for each
654 of these cubes, computed the temporal correlation matrix of the voxel responses during video
655 viewing. Specifically, for each of the 1976 volumes collected during video viewing, we correlated
656 the activity patterns in the given cube with the activity patterns (in the same cube) collected during
657 every other timepoint. This yielded a 1976 by 1976 correlation matrix for each cube.

658 Next, we constructed a series of “template” matrices: the first reflecting the timecourse of
659 video’s topic trajectory, and the others reflecting that of each participant’s recall topic trajectory.
660 To construct the video template, we computed the correlations between the topic proportions

estimated for every pair of TRs (prior to segmenting the trajectory into discrete events; i.e., the correlation matrix shown in Figs. 2B and 10A). We constructed similar temporal correlation matrices for each participant's recall topic trajectory (Figs. 2D, S4). However, to correct for length differences and potential non-linear transformations between viewing time and recall time, we first used dynamic time warping (Berndt and Clifford, 1994) to temporally align participants' recall topic trajectories with the video topic trajectory. An example correlation matrix before and after warping is shown in Fig. 10B. This yielded a 1976 by 1976 correlation matrix for the video template and for each participant's recall template.

To determine which (cubes of) voxel responses matched the video template, we correlated the upper triangle of the voxel correlation matrix for each cube with the upper triangle of the video template matrix (Kriegeskorte et al., 2008). This yielded, for each participant, a voxelwise map of correlation values. We then performed a one-sample *t*-test on the distribution of (Fisher *z*-transformed) correlations at each voxel, across participants. This resulted in a value for each voxel (cube), describing how reliably its timecourse mirrored that of the video.

We further sought to ensure that our analysis identified regions where the activations' temporal structure specifically reflected that of the video, rather than regions whose activity was simply autocorrelated at a width similar to the video template's diagonal. To achieve this, we used a phase shift-based permutation procedure, wherein we circularly shifted the video's topic trajectory by a random number of timepoints, computed the resulting "null" video template, and re-ran the searchlight analysis, in full. (For each of the 100 permutations, the same random shift was used for all participants). We *z*-scored the observed (unshifted) result at each voxel against the distribution of permutation-derived "null" results, and estimated a *p*-value by computing the proportion of shifted results that yielded larger values. To create the map in Figure 10A, we thresholded out any voxels whose similarity to the unshifted video's structure fell below the 95th percentile of the permutation-derived similarity results.

We used an analogous procedure to identify which voxels' responses reflected the recall templates. For each participant, we correlated the upper triangle of the correlation matrix for each cube of voxels with their (time warped) recall correlation matrix. As in the video template analysis this

689 yielded a voxelwise map of correlation coefficients per participant. However, whereas the video
690 analysis compared every participant's responses to the same template, here the recall templates
691 were unique for each participant. As in the analysis described above, we *t*-scored the (Fisher
692 *z*-transformed) voxelwise correlations, and used the same permutation procedure we developed
693 for the video responses to ensure specificity to the recall timeseries and assign significance values.
694 To create the map in Figure 10B we again thresholded out any voxels whose correspondence values
695 fell below the 95th percentile of the permutation-derived null distribution.

696 References

- 697 Atkinson, R. C. and Shiffrin, R. M. (1968). Human memory: A proposed system and its control
698 processes. In Spence, K. W. and Spence, J. T., editors, *The psychology of learning and motivation*,
699 volume 2, pages 89–105. Academic Press, New York.
- 700 Baldassano, C., Chen, J., Zadbood, A., Pillow, J. W., Hasson, U., and Norman, K. A. (2017).
701 Discovering event structure in continuous narrative perception and memory. *Neuron*, 95(3):709–
702 721.
- 703 Baldassano, C., Hasson, U., and Norman, K. A. (2018). Representation of real-world event schemas
704 during narrative perception. *Journal of Neuroscience*, 38(45):9689–9699.
- 705 Berndt, D. J. and Clifford, J. (1994). Using dynamic time warping to find patterns in time series. In
706 *KDD workshop*, volume 10, pages 359–370.
- 707 Blei, D. M. and Lafferty, J. D. (2006). Dynamic topic models. In *Proceedings of the 23rd International
708 Conference on Machine Learning*, ICML '06, pages 113–120, New York, NY, US. ACM.
- 709 Blei, D. M., Ng, A. Y., and Jordan, M. I. (2003). Latent dirichlet allocation. *Journal of Machine
710 Learning Research*, 3:993 – 1022.
- 711 Brunec, I. K., Moscovitch, M. M., and Barense, M. D. (2018). Boundaries shape cognitive represen-
712 tations of spaces and events. *Trends in Cognitive Sciences*, 22(7):637–650.

- 713 Bylinskii, Z., Isola, P., Bainbridge, C., Torralba, A., and Oliva, A. (2015). Intrinsic and extrinsic
714 effects on image memorability. *Vision Research*, 116:165–178.
- 715 Capota, M., Turek, J., Chen, P.-H., Zhu, X., Manning, J. R., Sundaram, N., Keller, B., Wang, Y., and
716 Shin, Y. S. (2017). Brain imaging analysis kit.
- 717 Cer, D., Yang, Y., Kong, S. Y., Hua, N., Limtiaco, N., John, R. S., Constant, N., Guajardo-Cespedes,
718 M., Yuan, S., Tar, C., Sung, Y.-H., Strope, B., and Kurzweil, R. (2018). Universal sentence encoder.
719 *arXiv*, 1803.11175.
- 720 Chen, J., Leong, Y. C., Honey, C. J., Yong, C. H., Norman, K. A., and Hasson, U. (2017). Shared
721 memories reveal shared structure in neural activity across individuals. *Nature Neuroscience*,
722 20(1):115.
- 723 Chun, M. and Turk-Browne, N. (2007). Interactions between attention and memory. *Current opinion
724 in neurobiology*, 17(2):177–184.
- 725 Clewett, D. and Davachi, L. (2017). The ebb and flow of experience determines the temporal
726 structure of memory. *Curr Opin Behav Sci*, 17:186–193.
- 727 Davachi, L. (2006). Item, context and relational episodic encoding in humans. *Current Opinion in
728 Neurobiology*, 16(6):693—700.
- 729 Davachi, L., Mitchell, J. P., and Wagner, A. D. (2003). Multiple routes to memory: distinct medial
730 temporal lobe processes build item and source memories. *Proceedings of the National Academy of
731 Sciences, USA*, 100(4):2157 – 2162.
- 732 Diana, R. A., Yonelinas, A. P., and Ranganath, C. (2007). Imaging recollection and famil-
733 iarity in the medial temporal lobe: a three-component model. *Trends in Cognitive Sciences*,
734 doi:10.1016/j.tics.2007.08.001.
- 735 Dobrushin, R. L. (1970). Prescribing a system of random variables by conditional distributions.
736 *Theory of Probability & Its Applications*, 15(3):458–486.

- 737 DuBrow, S. and Davachi, L. (2013). The influence of contextual boundaries on memory for the
738 sequential order of events. *Journal of Experimental Psychology: General*, 142(4):1277–1286.
- 739 Ezzyat, Y. and Davachi, L. (2011). What constitutes an episode in episodic memory? *Psychological
740 Science*, 22(2):243–252.
- 741 Friendly, M., Franklin, P. E., Hoffman, D., and Rubin, D. C. (1982). The Toronto Word Pool:
742 Norms for imagery, concreteness, orthographic variables, and grammatical usage for 1,080
743 words. *Behavior Research Methods and Instrumentation*, 14:375–399.
- 744 Gilboa, A. and Marlatte, H. (2017). Neurobiology of schemas and schema-mediated memory.
745 *Trends Cogn Sci*, 21(8):618–631.
- 746 Hasson, U., Chen, J., and Honey, C. J. (2015). Hierarchical process memory: memory as an integral
747 component of information processing. *Trends in Cognitive Science*, 19(6):304–315.
- 748 Hasson, U., Yang, E., Vallines, I., Heeger, D. J., and Rubin, N. (2008). A hierarchy of temporal
749 receptive windows in human cortex. *Journal of Neuroscience*, 28(10):2539–2550.
- 750 Heusser, A. C., Ezzyat, Y., Shiff, I., and Davachi, L. (2018a). Perceptual boundaries cause mnemonic
751 trade-offs between local boundary processing and across-trial associative binding. *Journal of
752 Experimental Psychology Learning, Memory, and Cognition*, 44(7):1075–1090.
- 753 Heusser, A. C., Fitzpatrick, P. C., Field, C. E., Ziman, K., and Manning, J. R. (2017). Quail: a
754 Python toolbox for analyzing and plotting free recall data. *The Journal of Open Source Software*,
755 10.21105/joss.00424.
- 756 Heusser, A. C., Ziman, K., Owen, L. L. W., and Manning, J. R. (2018b). HyperTools: a Python
757 toolbox for gaining geometric insights into high-dimensional data. *Journal of Machine Learning
758 Research*, 18(152):1–6.
- 759 Howard, M. W. and Kahana, M. J. (2002). A distributed representation of temporal context. *Journal
760 of Mathematical Psychology*, 46:269–299.

- 761 Howard, M. W., MacDonald, C. J., Tiganj, Z., Shankar, K. H., Du, Q., Hasselmo, M. E., and H., E.
762 (2014). A unified mathematical framework for coding time, space, and sequences in the medial
763 temporal lobe. *Journal of Neuroscience*, 34(13):4692–4707.
- 764 Howard, M. W., Viskontas, I. V., Shankar, K. H., and Fried, I. (2012). Ensembles of human MTL
765 neurons “jump back in time” in response to a repeated stimulus. *Hippocampus*, 22:1833–1847.
- 766 Huk, A., Bonnen, K., and He, B. J. (2018). Beyond trial-based paradigms: continuous behavior, on-
767 going neural activity, and naturalistic stimuli. *Journal of Neuroscience*, 10.1523/JNEUROSCI.1920-
768 17.2018.
- 769 Kahana, M. J. (1996). Associative retrieval processes in free recall. *Memory & Cognition*, 24:103–109.
- 770 Koriat, A. and Goldsmith, M. (1994). Memory in naturalistic and laboratory contexts: distin-
771 guishing accuracy-oriented and quantity-oriented approaches to memory assessment. *Journal of*
772 *Experimental Psychology: General*, 123(3):297–315.
- 773 Kriegeskorte, N., Mur, M., and Bandettini, P. (2008). Representational similarity analysis – con-
774 nnecting the branches of systems neuroscience. *Frontiers in Systems Neuroscience*, 2:1 – 28.
- 775 Landauer, T. K., Foltz, P. W., and Laham, D. (1998). Introduction to latent semantic analysis.
776 *Discourse Processes*, 25:259–284.
- 777 Lerner, Y., Honey, C. J., Silbert, L. J., and Hasson, U. (2011). Topographic mapping of a hierarchy
778 of temporal receptive windows using a narrated story. *Journal of Neuroscience*, 31(8):2906–2915.
- 779 Manning, J. R. (2019). Episodic memory: mental time travel or a quantum ‘memory wave’ function?
780 *PsyArXiv*, doi:10.31234/osf.io/6zjwb.
- 781 Manning, J. R., Norman, K. A., and Kahana, M. J. (2015). The role of context in episodic memory.
782 In Gazzaniga, M., editor, *The Cognitive Neurosciences, Fifth edition*, pages 557–566. MIT Press.
- 783 Manning, J. R., Polyn, S. M., Baltuch, G., Litt, B., and Kahana, M. J. (2011). Oscillatory patterns
784 in temporal lobe reveal context reinstatement during memory search. *Proceedings of the National*
785 *Academy of Sciences, USA*, 108(31):12893–12897.

- 786 McInnes, L., Healy, J., and Melville, J. (2018). UMAP: Uniform manifold approximation and
787 projection for dimension reduction. *arXiv*, 1802(03426).
- 788 Mikolov, T., Chen, K., Corrado, G., and Dean, J. (2013). Efficient estimation of word representations
789 in vector space. *arXiv*, 1301.3781.
- 790 Mueller, A., Fillion-Robin, J.-C., Boidol, R., Tian, F., Nechifor, P., yoonsubKim, Peter, Rampin, R.,
791 Corvellec, M., Medina, J., Dai, Y., Petrushev, B., Langner, K. M., Hong, Alessio, Ozsvald, I.,
792 vkolmakov, Jones, T., Bailey, E., Rho, V., IgorAPM, Roy, D., May, C., foobuzz, Piyush, Seong,
793 L. K., Goey, J. V., Smith, J. S., Gus, and Mai, F. (2018). WordCloud 1.5.0: a little word cloud
794 generator in Python. *Zenodo*, <https://zenodo.org/record/1322068#.W4tPKZNKh24>.
- 795 Murdock, B. B. (1962). The serial position effect of free recall. *Journal of Experimental Psychology*,
796 64:482–488.
- 797 Paller, K. A. and Wagner, A. D. (2002). Observing the transformation of experience into memory.
798 *Trends in Cognitive Sciences*, 6(2):93–102.
- 799 Pedregosa, F., Varoquaux, G., Gramfort, A., Michel, V., Thirion, B., Grisel, O., Blondel, M., Pretten-
800 hofer, P., Weiss, R., Dubourg, V., Vanderplas, J., Passos, A., Cournapeau, D., Brucher, M., Perrot,
801 M., and Duchesnay, E. (2011). Scikit-learn: Machine learning in Python. *Journal of Machine
802 Learning Research*, 12:2825–2830.
- 803 Polyn, S. M., Norman, K. A., and Kahana, M. J. (2009). A context maintenance and retrieval model
804 of organizational processes in free recall. *Psychological Review*, 116(1):129–156.
- 805 Postman, L. and Phillips, L. W. (1965). Short-term temporal changes in free recall. *Quarterly Journal
806 of Experimental Psychology*, 17:132–138.
- 807 Rabiner, L. (1989). A tutorial on Hidden Markov Models and selected applications in speech
808 recognition. *Proceedings of the IEEE*, 77(2):257–286.
- 809 Radvansky, G. A. and Zacks, J. M. (2017). Event boundaries in memory and cognition. *Curr Opin
810 Behav Sci*, 17:133–140.

- 811 Ramdas, A., Trillos, N., and Cuturi, M. (2017). On wasserstein two-sample testing and related
812 families of nonparametric tests. *Entropy*, 19(2):47.
- 813 Ranganath, C., Cohen, M. X., Dam, C., and D'Esposito, M. (2004). Inferior temporal, prefrontal,
814 and hippocampal contributions to visual working memory maintenance and associative memory
815 retrieval. *Journal of Neuroscience*, 24(16):3917–3925.
- 816 Ranganath, C. and Ritchey, M. (2012). Two cortical systems for memory-guided behavior. *Nature
817 Reviews Neuroscience*, 13:713 – 726.
- 818 Schlichting, M. L. and Preston, A. R. (2015). Memory integration: neural mechanisms and impli-
819 cations for behavior. *Current Opinion in Behavioral Sciences*, 1:1–8.
- 820 Simony, E., Honey, C. J., Chen, J., and Hasson, U. (2016). Uncovering stimulus-locked network
821 dynamics during narrative comprehension. *Nature Communications*, 7(12141):1–13.
- 822 Spalding, K. N., Schlichting, M. L., Zeithamova, D., Preston, A. R., Tranel, D., Duff, M. C., and
823 Warren, D. E. (2018). Ventromedial prefrontal cortex is necessary for normal associative inference
824 and memory integration. *The Journal of Neuroscience*, 38(15):3767–3775.
- 825 Stark, S. M., Yassa, M. A., and Stark, C. E. L. (2010). Individual differences in spatial pattern
826 separation performance associated with healthy aging in humans. *Learning & Memory*, 17(6):284–
827 288.
- 828 Steyvers, M., Shiffrin, R. M., and Nelson, D. L. (2004). Word association spaces for predicting
829 semantic similarity effects in episodic memory. In Healy, A. F., editor, *Cognitive Psychology and
830 its Applications: Festschrift in Honor of Lyle Bourne, Walter Kintsch, and Thomas Landauer*. American
831 Psychological Association, Washington, DC.
- 832 Tompry, A. and Davachi, L. (2017). Consolidation promotes the emergence of representational
833 overlap in the hippocampus and medial prefrontal cortex. *Neuron*, 96(1):228–241.
- 834 Tyng, C. M., Amin, H. U., Saad, M. N. M., and S, M. A. (2017). The influences of emotion on
835 learning and memory. *Frontiers in psychology*, 8:1454.

- 836 van Kesteren, M. T. R., Beul, S. F., Takashima, A., Henson, R. N., Ruiter, D. J., and Fernández, G.
837 (2013). Differential roles for medial prefrontal and medial temporal cortices in schema-dependent
838 encoding: from congruent to incongruent. *Neuropsychologia*, 51(12):2352–2359.
- 839 van Kesteren, M. T. R., Ruiter, D. J., Fernández, G., and Henson, R. N. (2012). How schema and
840 novelty augment memory formation. *Trends Neurosci*, 35(4):211–9.
- 841 Waskom, M., Botvinnik, O., Okane, D., Hobson, P., David, Halchenko, Y., Lukauskas, S., Cole, J. B.,
842 Warmenhoven, J., de Ruiter, J., Hoyer, S., Vanderplas, J., Villalba, S., Kunter, G., Quintero, E.,
843 Martin, M., Miles, A., Meyer, K., Augspurger, T., Yarkoni, T., Bachant, P., Williams, M., Evans,
844 Fitzgerald, C., Brian, Wehner, D., Hitz, G., Ziegler, E., Qalieh, A., and Lee, A. (2016). Seaborn:
845 v0.7.1.
- 846 Welch, G. B. and Burnett, C. T. (1924). Is primacy a factor in association-formation. *American Journal
847 of Psychology*, 35:396–401.
- 848 Wiltgen, B. J. and Silva, A. J. (2007). Memory for context becomes less specific with time. *Learning
849 & Memory*, 14(4):313–317.
- 850 Yassa, M. A., Lacy, J. W., Stark, S. M., Albert, M. S., Gallagher, M., and Stark, C. E. L. (2011). Pattern
851 separation deficits associated with increased hippocampal ca3 and dentate gyrus activity in
852 nondemented older adults. *Hippocampus*, 21(9):968–979.
- 853 Yassa, M. A. and Stark, C. E. L. (2011). Pattern separation in the hippocampus. *Trends In Neuro-
854 sciences*, 34(10):515–525.
- 855 Yonelinas, A. P. (2002). The nature of recollection and familiarity: A review of 30 years of research.
856 *Journal of Memory and Language*, 46:441–517.
- 857 Zacks, J. M., Speer, N. K., Swallow, K. M., Braver, T. S., and Reynolds, J. R. (2007). Event perception:
858 a mind-brain perspective. *Psychological Bulletin*, 133:273–293.
- 859 Zadbood, A., Chen, J., Leong, Y. C., Norman, K. A., and Hasson, U. (2017). How we transmit

860 memories to other brains: Constructing shared neural representations via communication. *Cereb*
861 *Cortex*, 27(10):4988–5000.

862 Zwaan, R. A. and Radvansky, G. A. (1998). Situation models in language comprehension and
863 memory. *Psychological Bulletin*, 123(2):162 – 185.

864 **Supporting information**

865 Supporting information is available in the online version of the paper.

866 **Acknowledgements**

867 We thank Luke Chang, Janice Chen, Chris Honey, Lucy Owen, Emily Whitaker, and Kirsten Ziman
868 for feedback and scientific discussions. We also thank Janice Chen, Yuan Chang Leong, Kenneth
869 Norman, and Uri Hasson for sharing the data used in our study. Our work was supported in part
870 by NSF EPSCoR Award Number 1632738. The content is solely the responsibility of the authors
871 and does not necessarily represent the official views of our supporting organizations.

872 **Author contributions**

873 Conceptualization: A.C.H. and J.R.M.; Methodology: A.C.H., P.C.F. and J.R.M.; Software: A.C.H.,
874 P.C.F. and J.R.M.; Analysis: A.C.H., P.C.F. and J.R.M.; Writing, Reviewing, and Editing: A.C.H.,
875 P.C.F. and J.R.M.; Supervision: J.R.M.

876 **Author information**

877 The authors declare no competing financial interests. Correspondence and requests for materials
878 should be addressed to J.R.M. (jeremy.r.manning@dartmouth.edu).